Organometallics **1993,** *12,* 738-743

Synthesis and Reactivity of $PdX[{}^tBu_2P(CH_2)_2CH(CH_2)_2P{}^tBu_2]$ (X = Cl, Me, H, BF_4)

Allen L. Seligson and William C. Trogler*

Department of Chemistry, 0506, University of California, San Diego,
La Jolla, California 92093-0506

Received August 17, 1992

The complex $PdCl[{}^tBu_2P(CH_2)_2CH(CH_2)_2P{}^tBu_2]$, **1**, is prepared conveniently by thermolysis of *trans*-$[Pd_2Cl_2\{\mu\text{-}{}^tBu_2P(CH_2)_5P{}^tBu_2\}_2]$ with a heat lamp. Electron-rich $PdCH_3[{}^tBu_2P(CH_2)_2CH(CH_2)P{}^tBu_2]$, **2**, and the unusually stable hydride analogue **3** form by metathesis of **1** with LiMe and $LiAlH_4$, respectively. Complex **2** crystallizes in the monoclinic space group $P2_1/c$ with $a = 12.334$ (6) Å, $b = 14.400$ (5) Å, $c = 14.993$ (6) Å, $\beta = 104.80$ (4)°, $V = 2575$ (2) Å^3, and $Z = 4$. Refinement of 3226 reflections with $I > 3\sigma(I)$ for 226 least-squares parameters converged to $R = 0.035$ and $R_w = 0.044$. The tridentate chelate in **2** adopts a syn double-bent conformation. The Pd–C distance to the chelated carbon lies closer to Pd [2.129 (4) Å] than does the trans methyl group [2.156 (5) Å]. Both the ^1H NMR (δ 2.22) and ^{13}C (δ 62.14) resonances for the chelate carbon lie unusually far downfield. Treatment of **2** with $[HNMe_3][BF_4]$ selectively protonates the CH_3 group and yields $Pd(BF_4)[{}^tBu_2P(CH_2)_2CH(CH_2)_2P{}^tBu_2]$, **5**. Even a weakly coordinating solvent, such as CH_2Cl_2, displaces the BF_4 ligand in **5**. In the presence of H_2O, the aquo complex $Pd(H_2O)[{}^tBu_2P(CH_2)_2CH(CH_2)_2P{}^tBu_2][BPh_4]$, **4**, was isolated. Complex **4** crystallizes in the monoclinic space group $P2_1/n$ with $a = 15.035$ (4) Å, $b = 19.110$ (6) Å, $c = 15.375$ (4) Å, $\beta = 90.85$ (2)°, $V = 4417$ (2) Å^3, and $Z = 4$. Refinement of 334 least-squares parameters for 3436 reflections of $I > 3\sigma(I)$ led to $R = 0.042$ and $R_w = 0.042$. The structure of **4** resembles that of **2** with the most noteworthy feature being the exceptionally long $Pd\text{–}OH_2$ distance of 2.301 (6) Å.

Introduction

The ligands coordinated to a transition metal greatly modify its reactivity. For soluble transition-metal catalysts, changing the ligands alters catalyst stability, reactivity, and selectivity. These effects have been quantified for phosphorus donor ligands by studies concerning the contribution of ligand steric and electronic parameters to reaction equilibra and rates.[1] Highly reactive catalysts often exhibit decreased selectivity and sometimes rapid loss of activity. Unfortunately, trends in catalyst activity and stability often oppose one another. Therefore, many ligand systems have been explored in trying to maximize catalytic activity, while retaining selectivity and a high activity.[2] In the course of a study to develop olefin amination catalysts with the general formula $PdR_2(PR_3)_2$, it became clear that an essential feature was the maintenance of a bis(phosphine)alkyl donor ligand set throughout the catalytic cycle. Furthermore, the tendency of Pd(II) compounds to form Pd(0) and deposit metal made it desirable to block reductive elimination pathways. A rigid $P\frown C\frown P$ donor chelate might fullfill these requirements.

Shaw and co-workers described the synthesis of several late-transition-metal complexes with the general formula $MCl_n[{}^tBu_2P(CH_2)_2CH(CH_2)_2P{}^tBu_2]$.[3,4] In these compounds the central carbon atom binds to the metal and forms two fused five-membered rings. An advantage of these compounds is the maintenance of a highly electron-rich set of donor ligands with a high thermal and oxidative stability. The rigid trans chelate also should help prevent alkane reductive elimination pathways. Such pathways often cause deposition of metal when late-transition-metal complexes are used in catalysis. This report describes the synthesis and reactivity of electron-rich complexes $PdX[{}^tBu_2P(CH_2)_2CH(CH_2)_2P{}^tBu_2]$, where X is chloride, methyl, and hydride. The following paper describes the application of the methyl derivative as a long-lived olefin amination catalyst.

Experimental Section

Materials. Reactions were performed under a nitrogen atmosphere by using modified Schlenk and glovebox techniques. Liquids were transferred by syringe (or cannula). Materials obtained from commercial sources were used without further purification, except where noted. Under a nitrogen atmosphere, Et_2O, benzene, and *n*-pentane were dried over Na–benzophenone ketyl. Methylene chloride and acetonitrile were distilled over

---

(1) Tolman, C. A. *Chem. Rev.* **1977,** *77,* 313.

(2) Parshall, G. W. Homogeneous Catalysis. *The Applications and Chemistry of Catalysis by Soluble Transition Metal Complexes;* John Wiley and Sons: New York, N.Y., 1980.

(3) (a) Al-Salem, N. A.; Empsall, H. D.; Markham, R.; Shaw, B. L.; Weeks, B. *J. Chem. Soc., Dalton Trans.* **1979,** 1972. (b) Al-Salem, N. A.; McDonald, W. S.; Markham, R.; Norton, M. C.; Shaw, B. L. *J. Chem. Soc., Dalton Trans.* **1980,** 59. (c) Briggs, J. R.; Constable, A. G.; McDonald, W. S.; Shaw, B. L. *J. Chem. Soc., Dalton Trans.* **1982,** 1225.

(4) (a) Crocker, C.; Empsall, H. D.; Errington, R. J.; Hyde, E. M.; McDonald, W. S.; Markham, R.; Norton, M. C.; Shaw, B. L.; Weeks, B. *J. Chem. Soc., Dalton Trans.* **1982,** 1217. (b) Errington, R. J.; McDonald, W. S.; Shaw, B. L. *J. Chem. Soc., Dalton Trans.* **1982,** 1829. (c) Crocker, C.; Errington, R. J.; Markham, R.; Moulton, C. J.; Odell, K. J.; Shaw, B. L. *J. Am. Chem. Soc.* **1980,** *102,* 4373. (d) Shaw, B. L. *J. Organomet. Chem.* **1980,** *200,* 307.

0276-7333/93/2312-0738$04.00/0

CaH_2. *trans*-bis[μ-1,5-bis(di-*tert*-butylphosphino)pentane]tetrachlorodipalladium(II) was synthesized according to a literature procedure.[3a]

Spectral Data. All NMR spectra were recorded on a GE QE-300 MHz FT NMR spectrometer equipped with a 5-mm broad-band probe. ^1H NMR chemical shifts were referenced to the residual solvent peak in the observed spectra. All $^{31}P\{^1H\}$ NMR spectra were referenced to the deuterated lock solvent, which had been previously referenced to 85% H_3PO_4. All $^{31}P\{^1H\}$ shifts were recorded relative to H_3PO_4, with downfield shifts being positive. IR spectra were recorded with the use of a Mattson Instruments Galaxy 2020 FT-IR spectrometer. Elemental analyses were performed by Onieda Research Services, Inc.

[1,5-Bis(di-*tert*-butylphosphino)pentan-3-yl-*C,P,P'*]chloropalladium(II), $PdCl[{}^tBu_2P(CH_2)_2CH(CH_2)_2P^tBu_2]$, 1. This compound has been previously reported by Shaw et al.,[3a] and a modified synthesis is reported here. *trans*-bis[μ-1,5-bis(di-*tert*-butylphosphino)pentane]tetrachlorodipalladium(II) (1.08 g, 1.00 mmol) was loaded into a sublimator and the pressure reduced to ~0.01 atm. The cold finger was cooled to −78 °C with dry ice, and the bottom of the sublimator was irradiated with a heat lamp. The sublimator was evacuated periodically to remove HCl gas formed by the reaction. White solid product was removed from the cold finger and the sides of the sublimator, dissolved in Et_2O (40 mL), and filtered to remove any traces of palladium metal decomposition product. The Et_2O solution was heated and reduced in volume until small crystals appeared. Colorless air-stable crystals of 1, 0.643 g (64%), formed on cooling to −35 °C.

[1,5-Bis(di-*tert*-butylphosphino)pentan-3-yl-*C,P,P'*]methylpalladium(II), $PdMe[{}^tBu_2P(CH_2)_2CH(CH_2)_2P^tBu_2]$, 2. Complex 1 (0.256 g, 0.51 mmol) was dissolved in Et_2O (20 mL). To this was added a solution of MeLi (0.365 mL, 1.4 M in Et_2O) and the solution was stirred for 1 h. Excess MeLi was hydrolyzed with degassed H_2O (5 mL), and the organic layer was removed. After the aqueous layer was washed with Et_2O (2 × 5 mL), the combined organic fractions were dried over $MgSO_4$. The colorless solution was filtered and the solvent removed. The remaining white solid was dissolved in pentane (10 mL) and the volume reduced to 3 mL. When cooled to −35 °C air-stable crystals of 2 formed: 0.213 g (84%); mp 165–175 °C dec; ^1H NMR (C_6D_6) 0.31 (t, $^3J_{PH}$ = 5 Hz, 3H, $PdCH_3$), 1.23 (q, $^3J_{PH}$ = 6 Hz, 36H, CCH_3), 1.60 (m, PCH_2CH_2), 1.99 (m, PCH_2CH_2), 2.22 (m, 1 H, PdC*H*); $^{13}C\{^1H\}$ (C_6D_6) 28.50 (t, PCH_2), 29.54 (s, $PCCH_3$), 29.93 (s, $PCCH_3$), 34.65 (t, PC), 36.01 (t, PC), 39.39 (t, PCH_2CH_2), 62.14 (s, PdCH); $^{31}P\{^1H\}$ (C_6D_6) 82.64 (s). Anal. Calcd for $C_{22}H_{48}P_2Pd$: C, 54.94; H, 10.06. Found: C, 55.03; H, 9.96. (Note: Dissolution of 2 in CD_2Cl_2 or $CDCl_3$ results in its slow conversion to 1).

[1,5-Bis(di-*tert*-butylphosphino)pentan-3-yl-*C,P,P'*]hydridopalladium(II), $PdH[{}^tBu_2P(CH_2)_2CH(CH_2)_2P^tBu_2]$, 3. To a solution of $LiAlH_4$ (0.008 g, 0.22 mmol) in THF (10 mL) was added a solution of complex 1 (0.1097 g, 0.22 mmol) in THF (10 mL). The colorless solution was stirred for 4 h, and it slowly turned pale yellow. The solvent was removed under vacuum and the residue extracted with pentane (3 × 10 mL). This solution was concentrated to ~1.5 mL and cooled at −35 °C to yield pale yellow crystals of 3: 0.076 g (75%); mp 135–170 °C dec; ^1H NMR (C_6D_6) −3.47 (td, $^3J_{PH}$ = 21 Hz, $^3J_{HH}$ = 3 Hz, 1H, Pd*H*), 1.24 (m, 36H, $PCCH_3$), 1.72 (m, PCH_2CH_2), 2.08 (m, PCH_2CH_2), 2.42 (m, 1H, PdC*H*); $^{31}P\{H\}$ NMR (C_6D_6) 105.85 (s). Anal. Calcd for $C_{21}H_{46}P_2Pd$: C, 54.02; H, 9.93. Found: C, 54.06; H, 9.73.

Aquo[1,5-bis(di-*tert*-butylphosphino)pentan-3-yl-*C,P,P'*]palladium(II) Tetraphenylborate, $[Pd(H_2O)[{}^tBu_2P(CH_2)_2CH(CH_2)_2P^tBu_2]][BPh_4]$, 4. A flask loaded with complex 2 (0.105 g, 0.22 mmol) and $[NH_2Et_2][BPh_4]$ (0.086 g, 0.22 mmol) was purged with ethylene for 3 min. To this was added C_6H_6 (10 mL), and the solution turned yellow. Continual purging of ethylene precipitated a white solid. The isolated solid was dissolved in CH_2Cl_2 (5 mL) and filtered. The yellow filtrate was concentrated to ~1 mL and layered with Et_2O (15 mL) to yield colorless air-stable crystals of 4: 0.093 g (53%) (the adventitious H_2O derives from the ethylene). Alternatively, the addition of $[NH_2Et_2][BPh_4]$ (0.006 g, 0.014 mmol) to complex 2 (0.007 g, 0.014 mmol) in CD_2Cl_2 (0.45 mL) with added H_2O (0.5 mL) yields 4 in quantitative yield by NMR: mp 133–135 °C dec; ^1H NMR (CD_2Cl_2) 1.26 (p, 36H, $PCCH_3$), 1.52 (m, PCH_2CH_2), 1.70 (m, PCH_2CH_2), 1.90 (m, PCH_2CH_2), 3.23 (tt, $^3J_{HH}$ = 12 Hz, $^3J_{PH}$ = 3 Hz, 1H, PdC*H*), 6.89 (t, 4H, C_6H_5), 7.04 (t, 8H, C_6H_5), 7.33 (m, 8H, C_6H_5); $^{13}C\{^1H\}$ NMR (CD_2Cl_2) 21.35 (t, PCH_2), 29.51 (s, $PCCH_3$), 29.75 (s, $PCCH_3$), 35.04 (t, PC), 36.20 (t, PC), 41.19 (t, PCH_2CH_2), 59.95 (s, PdCH), 122.38 (s, C_6H_5), 126.25 (s, C_6H_5), 136.18 (s, C_6H_5); $^{31}P\{^1H\}$ NMR (CD_2Cl_2) 87.13 (s); IR (KBr, cm^{-1}) 3495 (O–H). Anal. Calcd for $C_{45}H_{67}BOP_2Pd$: C, 67.29; H, 8.41. Found: C, 67.22; H, 8.32.

[1,5-Bis(di-*tert*-butylphosphino)pentan-3-yl-*C,P,P'*]palladium(II) Tetrafluoroborate, $[Pd[{}^tBu_2P(CH_2)_2CH(CH_2)_2P^tBu_2]][BF_4]$, 5. To a suspension of $[NHMe_3][BF_4]$ (0.042 g, 0.29) in toluene (2 mL) was added a solution of 2 (0.139 g, 0.29 mmol) in toluene (15 mL), and this mixture was refluxed under a nitrogen atmosphere for 3 h. On cooling the solution to room temperature, a white precipitate formed. The mixture was filtered, the solid residue dissolved in CH_2Cl_2 (5 mL), and the solution filtered. The pale yellow filtrate was concentrated to ~1.5 mL, layered with Et_2O (15 mL), and cooled to −35 °C to yield colorless crystals of 5: 0.087 g (54%). Complex 5 can be prepared more conveniently by oxidation. A solution of 2 (0.254 g, 0.53 mmol) was added to a suspension of $AgBF_4$ (0.103 g, 0.53 mmol) in CH_2Cl_2 (4 mL) and stirred for 0.5 h. The solution was filtered into a flask containing activated charcoal, stirred for 5 min, and then refiltered to yield a pale yellow solution. Concentration of the solution to 1.5 mL and layering with Et_2O (15 mL) yielded colorless crystals of 5: 0.241 g, (83%): 175–180 °C dec; ^1H NMR (CD_2Cl_2) 1.37 (p 36H, $PCCH_3$), 1.56 (m, PCH_2CH_2), 1.74 (m, PCH_2CH_2), 1.90 (m, PCH_2CH_2), 3.27 (tt, $^3J_{HH}$ = 12 Hz, $^3J_{PH}$ = 4 Hz, 1 H, PdC*H*); $^{31}P\{^1H\}$ NMR (CD_2Cl_2) 86.42 (s); IR (KBr, cm^{-1}) 2837, 2869, 2894, 2941, 2964, 2993 (C–H). Anal. Calcd for $C_{21}H_{45}BF_4P_2Pd$: C, 45.63; H, 8.21. Found: C, 45.52; H, 8.02.

X-ray Structure Determinations. X-ray crystallographic analyses were performed with the use of a Nicolet R3M/V automated diffractometer equipped with a graphite crystal monochromator and a Mo X-ray tube. Orientation matrix and unit cell parameters were determined by the least-squares fitting of 20 machine-centered reflections ($15° < 2\theta < 30°$) and confirmed by examination of axial photographs. Intensities of 3 check reflections were monitored every 197 reflections, throughout the data collection. Structure solutions and data workup were performed on a DEC Microvax II computer with SHELXTL PLUS version 3.4 software. Details on crystal and intensity data collection are given in Table I. Complete lists of atomic coordinates and bond distances and angles are available as supplementary material.

A colorless block-shaped crystal of 2, cut to the approximate dimensions 0.38 × 0.39 × 0.42 mm, was used for the room-temperature crystal and intensity data collection. The unit cell parameters and systematic absences $0k0$ ($k = 2k + 1$) and $h0l$ ($l = 2n + 1$) establish $P2_1/c$ as the space group. The structure was solved by direct methods. An absorption correction applied from ψ scan data did not significantly improve R, and therefore none was used. All non-hydrogen atoms were refined using anisotropic displacement parameters, and the hydrogen atoms were generated in idealized positions for the structure factor calculations but were not refined. Non-hydrogen atomic coordinates and isotropic displacements appear in Table II.

A colorless block-shaped crystal of 4, cut to the approximate dimensions 0.41 × 0.40 × 0.22 mm, was used for the crystal and intensity data collection at room temperature. The unit cell parameters and systematic absences $0k0$ ($k = 2k + 1$) and $h0l$ ($h + l = 2n + 1$) establish $P2_1/n$ as the space group. The structure was solved by direct methods. An absorption correction applied

Table I. Crystallographic Data and Summary of Data Collection and Refinement for Compounds 2 and 4 at 25 °C

	2	**4**
formula	$C_{22}H_{48}P_2Pd$	$C_{45}H_{67}BOP_2Pd$
fw	480.9	803.1
cryst syst	monoclinic	monoclinic
space group	$P2_1/c$	$P2_1/n$
a, Å	12.334 (6)	15.035 (4)
b, Å	14.400 (5)	19.110 (6)
c, Å	14.993 (6)	15.375 (4)
β, deg	104.80 (4)	90.85 (2)
V, Å^3	2575 (2)	4417 (2)
d_{calc}, g cm^{-3}	1.241	1.208
μ, mm^{-1}	0.837	0.515
scan type	Wyckoff	Wyckoff
no. of unique data	4647	5773
no. of rflns used, $I > 3\sigma(I)$	3226	3436
no. of params	226	334
Z	4	4
scan range, deg	$3.0 < 2\theta < 55.0$	$3.0 < 2\theta < 45.0$
largest residual peak, e/Å^3	0.29	0.45
R	0.035	0.042
R_w	0.044	0.042
GOF	1.02	1.54

Table II. Atomic Coordinates (×10^4) and Equivalent Isotropic Displacement Coefficients (Å^2 × 10^3) for 2

	x	y	z	U(eq)[a]
Pd(1)	7255 (1)	334 (1)	7171 (1)	33 (1)
P(1)	8616 (1)	857 (1)	6501 (1)	38 (1)
P(2)	5971 (1)	−522 (1)	7691 (1)	37 (1)
C(1)	7111 (4)	1586 (3)	7921 (3)	60 (2)
C(2)	8705 (5)	−70 (4)	5667 (3)	60 (2)
C(3)	8277 (5)	−972 (4)	5969 (3)	65 (2)
C(4)	7212 (4)	−822 (3)	6277 (3)	47 (2)
C(5)	6797 (5)	−1720 (3)	6609 (3)	63 (2)
C(6)	5751 (5)	−1562 (3)	6957 (3)	58 (2)
C(7)	8286 (4)	1910 (3)	5737 (3)	56 (2)
C(8)	7019 (5)	1835 (5)	5277 (4)	83 (3)
C(9)	8924 (6)	1953 (5)	4983 (4)	87 (3)
C(10)	8490 (6)	2808 (4)	6291 (4)	82 (3)
C(11)	10061 (4)	941 (4)	7298 (3)	55 (2)
C(12)	10368 (6)	−55 (5)	7675 (5)	91 (3)
C(13)	10056 (5)	1575 (5)	8112 (4)	89 (3)
C(14)	10964 (5)	1265 (5)	6841 (4)	84 (3)
C(15)	4517 (4)	−15 (3)	7479 (3)	49 (2)
C(16)	4449 (5)	699 (4)	8226 (4)	69 (2)
C(17)	4322 (5)	487 (4)	6543 (4)	75 (2)
C(18)	3581 (5)	−731 (4)	7411 (5)	78 (3)
C(19)	6469 (5)	−976 (4)	8907 (3)	64 (2)
C(20)	7457 (5)	−1617 (5)	8929 (4)	93 (3)
C(21)	5595 (6)	−1537 (5)	9235 (4)	90 (3)
C(22)	6888 (6)	−174 (5)	9567 (3)	88 (3)

[a] Equivalent isotropic U defined as one-third of the trace of the orthogonalized U_{ij} tensor.

Table III. Atomic Coordinates (×10^4) and Equivalent Isotropic Displacement Coefficients (Å^2 × 10^3) for 4

	x	y	z	U(eq)[a]
O(1)	2161 (6)	7137 (4)	7877 (3)	64 (2)
Pd(1)	2032 (1)	7111 (1)	9366 (1)	42 (1)
P(1)	1893 (1)	8315 (1)	9553 (1)	48 (1)
P(2)	2157 (1)	5898 (1)	9519 (1)	48 (1)
C(3)	1595 (5)	8391 (4)	10703 (4)	70 (3)
C(4)	1915 (6)	7737 (4)	11160 (4)	77 (4)
C(5)	1708 (5)	7075 (4)	10659 (4)	63 (3)
C(6)	2025 (6)	6438 (5)	11138 (5)	96 (4)
C(7)	1842 (5)	5766 (4)	10652 (4)	78 (3)
C(10)	2951 (4)	8807 (4)	9409 (4)	57 (3)
C(11)	2864 (6)	9605 (4)	9461 (5)	90 (4)
C(12)	3576 (5)	8588 (5)	10142 (5)	92 (4)
C(13)	3369 (5)	8591 (4)	8553 (4)	72 (3)
C(20)	950 (5)	8733 (4)	8948 (5)	59 (3)
C(21)	610 (6)	9402 (4)	9380 (5)	99 (4)
C(22)	1181 (5)	8886 (4)	8003 (5)	76 (3)
C(23)	195 (5)	8202 (4)	8948 (5)	85 (4)
C(30)	1331 (4)	5381 (3)	8882 (5)	58 (3)
C(31)	3876 (5)	5855 (5)	10116 (6)	109 (4)
C(32)	467 (4)	5817 (4)	8891 (5)	75 (3)
C(33)	1131 (5)	4658 (4)	9263 (6)	95 (4)
C(40)	3304 (5)	5539 (4)	9393 (5)	64 (3)
C(41)	1599 (5)	5299 (4)	7934 (5)	73 (3)
C(42)	3676 (5)	5783 (4)	8529 (6)	93 (4)
C(43)	3372 (5)	4745 (4)	9463 (5)	81 (3)
B(1)	8022 (4)	2856 (4)	5012 (4)	45 (2)
C(50)	7133 (4)	2885 (3)	4387 (3)	43 (1)
C(51)	6798 (4)	2283 (3)	3997 (4)	59 (2)
C(52)	6069 (5)	2284 (4)	3429 (4)	66 (2)
C(53)	5653 (4)	2898 (4)	3219 (4)	67 (2)
C(54)	5972 (5)	3495 (4)	3557 (5)	68 (2)
C(55)	6686 (4)	3499 (4)	4135 (4)	54 (2)
C(60)	7997 (4)	2185 (3)	5679 (4)	42 (1)
C(61)	7209 (4)	1873 (3)	5958 (4)	55 (2)
C(62)	7196 (5)	1335 (4)	6566 (4)	61 (2)
C(63)	7978 (4)	1086 (4)	6901 (4)	59 (2)
C(64)	8765 (4)	1370 (3)	6660 (4)	56 (2)
C(65)	8772 (4)	1918 (3)	6069 (4)	53 (2)
C(70)	8848 (3)	2831 (3)	4335 (3)	42 (1)
C(71)	9297 (4)	2222 (3)	4097 (4)	53 (2)
C(72)	9969 (4)	2211 (4)	3489 (4)	63 (2)
C(73)	10234 (4)	2807 (4)	3103 (4)	63 (2)
C(74)	9825 (4)	3413 (4)	3295 (4)	64 (2)
C(75)	9128 (4)	3430 (3)	3891 (4)	58 (2)
C(80)	8113 (4)	3539 (3)	5668 (4)	46 (2)
C(81)	8908 (5)	3854 (4)	5890 (4)	67 (2)
C(82)	8991 (5)	4401 (4)	6484 (5)	79 (2)
C(83)	8260 (5)	4661 (4)	6861 (5)	70 (2)
C(84)	7456 (5)	4369 (4)	6683 (4)	71 (2)
C(85)	7377 (5)	3820 (4)	6090 (4)	62 (2)

[a] Equivalent isotropic U defined as one-third of the trace of the orthogonalized U_{ij} tensor.

from ψ scan data did not significantly improve R, and therefore none was used. All non-hydrogen atoms were refined using anisotropic displacement parameters. The phenyl groups of the BPh_4 anion were all treated as rigid groups with isotropic displacement parameters for each carbon. The hydrogen atoms were generated in idealized positions for the structure factor calculations but were not refined. The exception was H(1A) and H(1B) for the bound water, which were located in the Fourier difference maps and refined. Non-hydrogen atomic coordinates and isotropic coordinates for 4 appear in Table III.

Results and Discussion

Preparation and Reactivity of 1. Complex 1 was first reported as a byproduct from the reaction between $PdCl_2(PhCN)_2$ and $^tBu_2P(CH_2)_5P^tBu_2$ in low yield.[3a] The main product of this reaction, *trans*-$[Pd_2Cl_4\{^tBu_2P(CH_2)_5P^tBu_2\}_2]$, decomposes at 260 °C to yield 1 (eq 1). To synthesize 1 on a larger scale, *trans*-$[Pd_2Cl_4\{\mu\text{-}^tBu_2P(CH_2)_5P^tBu_2\}_2]$ is placed in a sublimator and irradiated with a heat lamp and 1 collected by sublimation. The tridentate chelate provides a rigid ligand backbone, which results in a high thermal stability for 1.

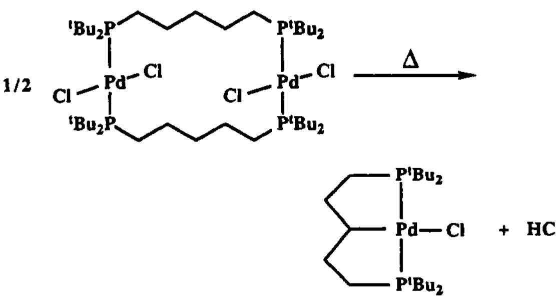

1

(1)

The reaction between 1 and MeLi yields the new palladium dialkyl species 2 (eq 2). This compound crystallizes in good yield and is air-stable. A singlet resonance in the $^{31}\mathrm{P}\{^1\mathrm{H}\}$ NMR spectrum of 2 establishes the equivalent phosphines, and suggests a trans geometry. In the ^{1}H NMR spectrum of 2 the palladium-methyl resonance at 0.31 ppm appears as a triplet from coupling with the mutually trans phosphines. This chemical shift falls in the same region as other previously reported palladium alkyls.[5] The hydrogen bound to the metalated chelate carbon appears as a multiplet coupled to the two phosphines and the neighboring methylenes. This resonance occurs downfield at 2.22 ppm, an uncharacteristic low-field shift for palladium alkyls. The $^{13}\mathrm{C}\{^1\mathrm{H}\}$ spectrum of 2 also shows the Pd–^{13}CH< resonance unusually far downfield at δ 62.14. This is more than 20 ppm downfield from all the other ^{13}C resonances in the spectrum.

(2)

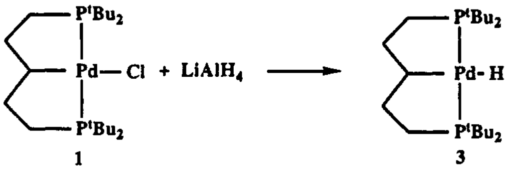

(3)

In a similar reaction, 1 combines with $\mathrm{LiAlH_4}$ to yield the palladium-hydrido alkyl complex 3 (eq 3). The ligation of hydride was established by its characteristic resonance at −3.47 ppm in the ^{1}H NMR spectrum. This resonance appears as a triplet of doublets, split by the phosphines and the proton on the chelate carbon trans to it. This remarkably stable hydrido-alkyl complex can be heated above 100 °C without decomposition. Palladium hydrido alkyls are rarely stable to reductive elimination at room temperature and rapidly decompose to yield alkane.[6] The rigidity of the chelated alkyl-phosphine backbone in 3 locks the complex in the trans configuration. This prevents trans to cis isomerization, which is a necessary step for intramolecular reductive elimination of alkane.[7] Steric hindrance from the bulky ligand also should block intermolecular elimination pathways.

Reactivity of Complex 2. Protonolysis of late-metal-alkyl bonds by weak acids in other complexes[8,9] led us to explore the reactivity of 2. The reaction of 2 with $\mathrm{[HNMe_3][BF_4]}$ rapidly cleaves the palladium-methyl bond (eq 4) to yield 5. The proton NMR spectrum shows no resonances from coordinated trimethylamine! This contrasts with the analogous reaction of $\mathrm{Pd(CH_3)_2(dmpe)}$, which forms a stable $\mathrm{NMe_3}$ complex.[9] The connectivity of remaining ligands coordinated to palladium in 5 must be the same as in the starting material, because of their similar chemical shifts. The distinct proton resonance for the palladium-bound carbon shifts even further downfield to 3.23 ppm. A singlet appears in the ^{31}P NMR spectrum at 86.24 ppm, also shifted downfield from the resonance of 2. This resonance shifts and splits on lowering the temperature.

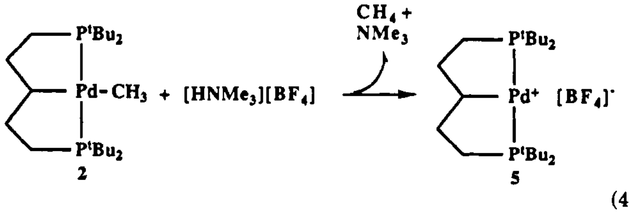

(4)

At −70 °C the ^{31}P NMR spectrum of 5 exhibits two new resonances at 85.17 and 84.53 ppm in a 1.3:1 ratio by integrated intensity (1.8:1 by peak height) ratio. Warming the solution to −30 °C resulted in coalescence of the two peaks. We tentatively attribute these resonances to an equilibrium between the $\mathrm{BF_4^-}$ complex and a solvent adduct. Coordination of fluorine lone pairs ($\mathrm{BF_4^-}$, A) or the solvent chlorine ($\mathrm{CH_2Cl_2}$, B) to the open coordination site of 5 must be strong enough to freeze out their equilibration below −30 °C. Halocarbon–metal binding has precedent in other Lewis-acidic transition-metal systems.[10] Elemental analysis of crystalline 5 establishes the absence of $\mathrm{CH_2Cl_2}$ in the solid state. X-ray-quality crystals of 5 were grown, but they decompose rapidly in the X-ray beam.

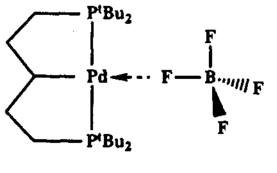

A

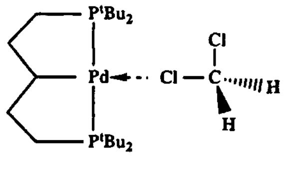

B

Protonolysis of 2 with $\mathrm{[NH_2Et_2][BF_4]}$ in wet $\mathrm{CH_2Cl_2}$ produces the palladium aquo complex 4, as shown in eq 5. The ^{1}H and ^{31}P NMR spectra of 4 resemble those of 5; however, this complex displays a sharp O–H stretching peak at 3495 cm^{-1} in the IR spectrum. The X-ray crystal structure of 4 confirms this assignment. The reaction between 4 and the strong base $\mathrm{LiN(SiMe_3)_2}$ in $\mathrm{CD_2Cl_2}$ resulted in an immediate change in the ^{1}H and ^{31}P NMR spectra. The resonance of the proton bound to the chelated palladium-alkyl shifted downfield to 3.64 ppm and the ^{31}P NMR singlet shifted to 88.05 ppm. This new species formed may correspond to the deprotonated form of 5, a hydroxide complex. Several late-transition-metal hy-

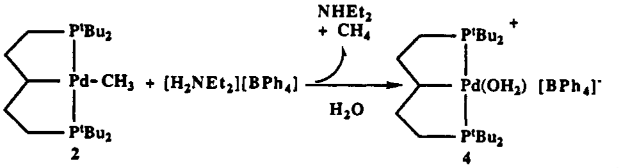

(5)

---

(5) (a) Tooze, R.; Chiu, K. W.; Wilkinson, G. *Polyhedron* **1984**, *3*, 1025. (b) Ito, T.; Tsuchtya, H.; Yamamoto, A. *Bull. Chem. Soc. Jpn.* **1977**, *50*, 1319. (c) Ozawa, F.; Ito, T.; Nakamura, Y.; Yamamoto, A. *Bull. Chem. Soc. Jpn.* **1981**, *54*, 1868.

(6) Abis, L.; Santi, R.; Halpern, J. *J. Organomet. Chem.* **1981**, *215*, 263.

(7) Collman, J. P.; Hegedus, L. S.; Norton, J. R.; Finke, R. G. *Principles and Applications of Organotransition Metal Chemistry*; University Science Books: Mill Valley, CA, 1987.

(8) (a) Kim, Y.-H.; Osakada, K.; Takenaka, A.; Yamamoto, A. *J. Am. Chem. Soc.* **1990**, *112*, 1096. (b) Osakada, K.; Kim, Y.-J.; Tanaka, M.; Ishiguro, S.; Yamamoto, A. *Inorg. Chem.* **1991**, *30*, 197. (c) Lundquist, E. G.; Folting, K.; Huffman, J. C.; Caulton, K. G. *Organometallics* **1990**, *9*, 2254.

(9) (a) Seligson, A. L.; Trogler, W. C. *Inorg. Chem.* **1991**, *30*, 3371. (b) Seligson, A. L.; Trogler, W. C. *J. Am. Chem. Soc.* **1991**, *113*, 2520.

(10) Kulawiec, R. J.; Crabtree, R. H. *Coord. Chem. Rev.* **1990**, *99*, 89. Agbossou, S. K.; Roger, C.; Igau, A.; Gladysz, J. A. *Inorg. Chem.* **1992**, *31*, 419. Van Seggen, D. M.; Anderson, O. P.; Strauss, S. H. *Inorg. Chem.* **1992**, *31*, 2987, and references therein.

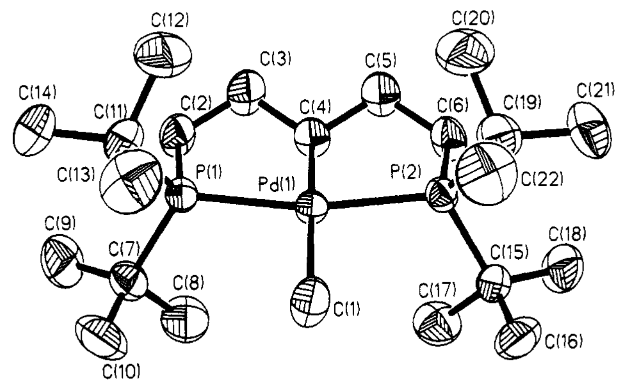

Figure 1. Thermal ellipsoid plot at 50% probability for 2.

Table IV. Selected Bond Distances (Å) and Angles (deg) for 2

Pd(1)–P(1)	2.293 (2)	Pd(1)–P(2)	2.294 (2)
Pd(1)–C(1)	2.156 (5)	Pd(1)–C(4)	2.129 (4)
C(3)–C(4)	1.515 (8)	C(4)–C(5)	1.521 (7)
P(1)–Pd(1)–P(2)	166.2 (1)	P(1)–Pd(1)–C(1)	96.9 (2)
P(2)–Pd(1)–C(1)	96.7 (2)	P(1)–Pd(1)–C(4)	83.3 (1)
P(2)–Pd(1)–C(4)	83.4 (1)	C(1)–Pd(1)–C(4)	171.9 (2)
Pd(1)–C(4)–C(3)	114.8 (3)	Pd(1)–C(4)–C(5)	114.5 (3)
C(3)–C(4)–C(5)	111.64		

Table V. Selected Bond Distances (Å) and Angles (deg) for 4

O(1)–Pd(1)	2.301 (6)	Pd(1)–P(1)	2.329 (2)
Pd(1)–P(2)	2.338 (2)	Pd(1)–C(5)	2.056 (6)
C(4)–C(5)	1.510 (11)	C(5)–C(6)	1.496 (12)
O(1)–H(1A)	0.73 (9)	O(1)–H(1B)	0.66 (8)
O(1)–Pd(1)–P(1)	96.3 (2)	O(1)–Pd(1)–P(2)	96.5 (2)
P(1)–Pd(1)–P(2)	167.1 (1)	O(1)–Pd(1)–C(5)	171.1 (3)
P(1)–Pd(1)–C(5)	83.7 (2)	P(2)–Pd(1)–C(5)	83.7 (2)
Pd(1)–C(5)–C(4)	114.5 (5)	Pd(1)–C(5)–C(6)	115.1 (5)
C(4)–C(5)–C(6)	111.7 (6)	H(1A)–O(1)–H(1B)	100 (9)

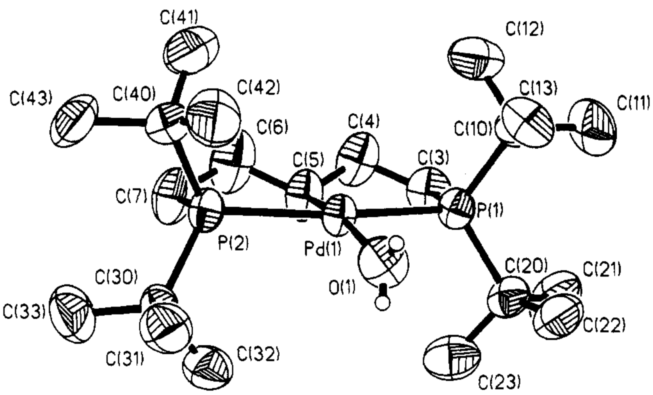

Figure 2. Thermal ellipsoid plot at 50% probability for 4.

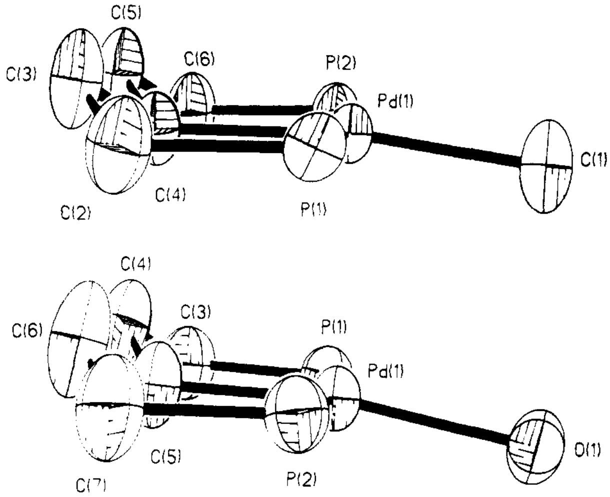

Figure 3. Plots showing the double-bent chelate ring conformation in 2 (top) and 4 (bottom), as well as the downward displacement of the trans ligand in both complexes.

droxide complexes have been reported.[11] At longer times the deprotonated complex reacts with CD_2Cl_2 to form 1.

Crystal Structure Determination of 2 and 4. Complex 2 exhibits a trans square-planar geometry, shown in Figure 1. Table IV contains selected bond distances and angles. The chelate distorts the complex slightly away from an ideal square-planar geometry by pinching back the two phosphines away from the methyl group. This results in a P(1)–Pd(1)–P(2) bond angle of 166.2 (1)°. The palladium–carbon bond of the metallated chelate is 0.027 (9) Å shorter than the palladium–methyl bond. These distances are slightly longer than the palladium–methyl bond lengths in $Pd(dmpe)Me_2$.[12] This may be attributed to the greater trans effect of carbon as compared to phosphorus.[13]

Figure 2 shows the square-planar structure of the cationic palladium(II) complex 4. Table V contains selected bond distances and angles. Complex 4 exhibits a similar distortion of the P(1)–Pd(1)–P(2) bond angle as in 2. This molecule also deviates from a planar geometry. The O(1)–Pd(1)–C(5) bond angle of 171.1 (3)° drops the oxygen atom below the plane formed by the palladium, phosphines, and the metalated alkyl, similar to the methyl group in 2 (Figure 3). The palladium–oxygen distance of 2.301 (6) Å is extremely long. This bond is 0.1 Å longer than the Pd–O bond length in the complex $[Pd(H)(PCy_3)_2(H_2O)][BF_4]$.[14] It is doubtful that the differences in trans effect between a hydride and an alkyl would cause this increased bond distance, since hydride is a stronger trans-directing ligand than an alkyl.[13] A more likely explanation is that severe steric crowding in 4 prevents even small ligands (e.g., CH_3, H_2O) from optimal binding in the square plane. This may help explain the high reactivity of the CH_3 group in 2 relative to the chelated alkyl.

The hydrogen atoms bound to water in 4 were located in the Fourier difference maps, and the O–H distances were found to be 0.73 (9) and 0.66 (8) Å, which is shorter than the internuclear separation in water of 0.958 (4) Å. The shortening of X-ray-determined bond lengths to hydrogen is well recognized.[15] The plane of the bound water lies perpendicular to the $\widehat{PCP}$ plane of the chelate. The geometry of H_2O appears not to be highly distorted by its complexation to palladium, since the H(1A)–O(1)–H(1B) bond angle of 100 (9)° is statistically about the same as in water (104.5°).

In both 2 and 4 (Figure 3) the 1,6-diphospha-7-pallada-[3.3.0]bicyclooctane ring system adopts a double-bent conformation. Six of these atoms lie nearly in a plane.

---

(11) (a) Milstein, D.; Calabrese, J. C.; Williams, I. D. *J. Am. Chem. Soc.* **1986**, *108*, 6387. (b) Bennett, M. A.; Yoshida, T. *J. Am. Chem. Soc.* **1978**, *100*, 1750. (c) Appleton, T. G.; Bennett, M. A. *Inorg. Chem.* **1978**, *17*, 738. (d) Bryndza, H. E.; Tam, W. *Chem. Rev.* **1988**, *88*, 1163.

(12) Graff, W.; Boersma, J.; Smeets, W. J.; Speck, A. L.; van Koten, G. *Organometallics* **1989**, *8*, 2907.

(13) Huheey, J. E. *Inorganic Chemistry: Principles of Structure and Reactivity*, 3rd ed.; Harper and Row Publishers, Inc.: New York, NY, 1983.

(14) Leoni, P.; Sommovigo, M.; Pasquali, M.; Midollini, S.; Braga, D.; Sabitino, P. *Organometallics* **1991**, *10*, 1038.

(15) Churchill, M. R. *Inorg. Chem.* **1973**, *12*, 1213.

Table VI. ¹H and ¹³C{¹H} NMR Chemical Shifts of the Palladium-Bound Chelate Moiety

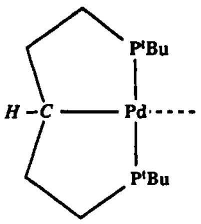

complex	¹H NMR chem shift (ppm)	¹³C{¹H} chem shift (ppm)
1[a]	2.58	62.14
2[a]	2.22	57.53
3[a]	2.42	
4[b]	3.23	59.95
5[b]	3.27	

[a] Solvent = C_6D_6. [b] Solvent = CD_2Cl_2.

A perpendicular pseudo-mirror plane bisects the chelate ring system. The methylene groups C(3) and C(5) in **2** and C(4) and C(6) in **4** lie displaced from the plane in the same direction. This appears to cause a difference in the positioning of the *tert*-butyl substituents on P(1) and P(2) with respect to the two faces of the square plane. Methyl groups lie above the region of the trans ligand (C(22) and C(13) in **2** and C(42) and C(13) in **4**). This forces the trans ligand downward toward the less congested side of the square plane. The ¹³C{¹H} NMR spectra for **2** and **4** show separate resonances for *tert*-butyl substituents, which suggests this structural feature persists in solution.

The palladium–carbon bond distance to the chelate carbon decreases from 2.129 (4) Å in complex **2** to 2.056 (6) in **4**. This decrease in bond length could be attributed to increased palladium–carbon double-bond character as the trans ligand becomes a weaker donor. This bond distance lies between the iridium–carbon double-bond length of 2.00 Å in the carbene complex $Ir[{}^tBu_2P(CH_2)_2C(CH_2)_2P^tBu_2]$[4a] and **2**. It is interesting that the angle made by the metalated carbon and its neighboring methylenes is 111° in all three complexes. This parameter does not gauge carbene character. The decrease in the palladium–carbon bond distance also results in downfield shifts of the ¹³C resonance, and of the ¹H NMR resonance of the proton bound to that carbon. These phenomena may result from a slight change in hybridization of the carbon atom from sp³ to sp². Table VI summarizes these chemical shifts. For **2** a $J_{^{13}C-H}$ of ~120 Hz was determined from the proton–carbon 2DJ spectrum. This represents a normal value for an sp³ carbon atom and does not support the hypothesis that partial carbene character causes the unusual chemical shift of the chelating C–H group. The normal coupling, however, may reflect the constancy of the bond angles in the metallabicycle ring.

Conclusions

The chloride ligand in **1** substitutes readily to yield the corresponding methyl and hydrido palladium alkyl complexes. The palladium hydrido alkyl **3** shows a remarkably enhanced stability toward reductive elimination over other such complexes.[6] The palladium dialkyl **2**, exhibits basicity characteristics similar to $Pd(dmpe)R_2$ complexes.[8,9] Protonolysis of **2** with ammonium salts exclusively cleaves the palladium–methyl bond, and the palladium–alkyl bond of the chelate chain remains inert. The X-ray crystal structure analysis of **2** shows that this palladium–alkyl bond is about 0.02 Å shorter than the palladium–methyl bond distance. This, along with the greater steric constraints of the chelated palladium–alkyl bond, may account for selective protonlysis of the trans methyl ligand. These reactivity properties are crucial for the application of **2** as a long-lived olefin amination catalyst (see following paper).

Unexpectedly, the reaction of **2** with ammonium salts yields **5** and not the corresponding cationic amine complexes. The steric bulk of *tert*-butyl groups on the phosphine apparently blocks coordination of an amine. The BF_4^- counterion in **5** appears to only weakly associate with the palladium center, so that even CH_2Cl_2 solvent can behave as a ligand. The less sterically demanding ligand water binds weakly to form **4**.

Acknowledgment. This work was supported by the National Science Foundation (Grant No. CHE-88015958). We thank Dr. John Wright for measuring the 2DJ spectrum of **2**.

Supplementary Material Available: Tables of crystal data, bond distances, bond angles, hydrogen atom positions, and thermal parameters for **2** and **4** (17 pages). Ordering information is given on any current masthead page.

OM9205049